Electronic Supplementary Material (ESI) for RSC Advances.

Discovery of hydrazide based pyridazino[4,5-*b*]indole scaffold as a new phosphoinositide 3-kinase (PI3K) inhibitors for breast cancer therapy

Ahmed A. M. Sarhan[a,*], Ahmed T. A. Boraei[b], Assem Barakat [c,d], Mohamed S. Nafie[b,*]

[a.] Chemistry Department, Faculty of Science, Arish University, Al-Arish 45511, Egypt ahmed_sarhan252@yahoo.com

[b.] Chemistry Department, Faculty of Science, Suez Canal University, Ismailia 41522, Egypt.

[c.] Chemistry Department, College of Science, King Saud University, P.O. Box 2455, Riyadh 11451, Saudi Arabia. *ambarakat@ksu.edu.sa*

[d.] Chemistry Department, Faculty of Science, Alexandria University, P.O. Box 426, Ibrahimia, Alexandria 21321, Egypt

† Author to whom correspondence should be addressed; E-Mail: ahmed_sarhan252@yahoo.com (A.A.M.S.); Mohamed_nafie@science.suez.edu.eg (M.S.N.)

1.1. Materials and Methods

1.1. General

Melting points are determined using a melting-point apparatus (SMP10) in open capillaries and are uncorrected. The progress of the reactions was monitored by thin layer chromatography (Merck). Detections were achieved by UV light illumination. For flash chromatography commercial silica was used. Nuclear magnetic resonance (^{1}H NMR, ^{13}C NMR and 2D NMR) spectra were determined in DMSO-d_6 and were recorded on Bruker AC 300-500 spectrometers using TMS as an internal standard. Chemical shifts are termed in δ (ppm) and coupling constants are described in Hz. The assignment of exchangeable O*H* and N*H* was confirmed by D_2O. CHNS-microanalysis was done using Flash EA-1112 instrument.

1.2. Biological evaluation

1.2.1. Cytotoxic screening using MTT assay

Using the MTT assay [1], cytotoxic efficacy of the tested derivatives was done against breast cancer (MCF-7) and liver cancer (HepG2) cell lines and normal GMSC cell line. Each cell line was cultured in a proper complete medium composed of RPMI-1640 or DMEM, respectively, supplemented with 10% fetal bovine serum, and 1% Antibiotic (Penicillin/Streptomycin (1:1)) according to the standard cell culture work [2]. Cells were treated for 48 h with four working concentrations of compounds (1, 10, 100, and 1000 μM). The experiment was conducted six times. Data were calculated as percent of cell viability by the following formula: % cell viability = (Mean absorbance in test wells / Mean absorbance in control wells) x 100, then IC_{50} was calculated were determined using Graph Pad Prism 7.0 [3].

1.2.2. RT-PCR

Based on the significant cytotoxic activity of the studied derivatives, compound **12** (IC_{50} = 4.25 μM) was thought worthwhile to further investigate its effect on induction of apoptosis in MCF-7 cancer cells. MCF-7 cells were treated with DMSO (control) and compound **12** (5 μM- treated) for 48 h. Total RNA was extracted from both treated and non-treated cells using Qiagen RNA extraction. The purity of RNA was recorded using nanodrop spectrophotometer. cDNA synthesis was done, then subsequent qPCR test was performed in a single tube [21]. The primers sequence used in the RT-PCR test were provided through the supplementary online material. The results obtained were expressed in cycle threshold (Ct), and relative quantitation of each tested gene was assessed according to the calculation of delta-delta Ct.

1.3. *In silico*

All molecular modeling studies were conducted on a computational software basis using the Molecular Operating Environment (MOE 2008-10 Chemical Computing Group, Canada). For the docking studies, the crystal structure of phosphoinositide 3-kinase inhibition was obtained from the Protein data bank (PDB code: 1e7V) [18]. Methodology regarding ligand and receptor preparation and optimization was carried out according to Nafie el.al [4]. Each ligand-receptor complex was tested for interaction analysis, 2D images were made using the MOE visualizing tool, and 3D images were taken by Chimera as a visualizing software.

References

1. T. Mosmann, Journal of Immunological Methods. 1983, **65**, 55–63.
2. R. Ian. Freshney, Culture of animal cells: a manual of basic technique and specialized applications, Wiley-Blackwell, Hoboken, N.J., 2010.
3. A.I. Khodair, M.A. Alsafi, M.S. Nafie, Carbohydrate Research. 2019, **486**, 107832.
4. M.S. Nafie, M.A. Tantawy, G.A. Steroids. 2019**, 152**, 108485.

Table S1: Summarized ligand-receptor interactions for the lead derivatives with 2D and 3D representation

Compound	Binding affinity (Kcal/mol)	Type of interaction	Bond length (Aº)	Interaction moiety involved	Amino acid
Co-crystallized ligand	**-11.76**	**H-acceptor**	**1.55**	**-O-**	**Val 882**
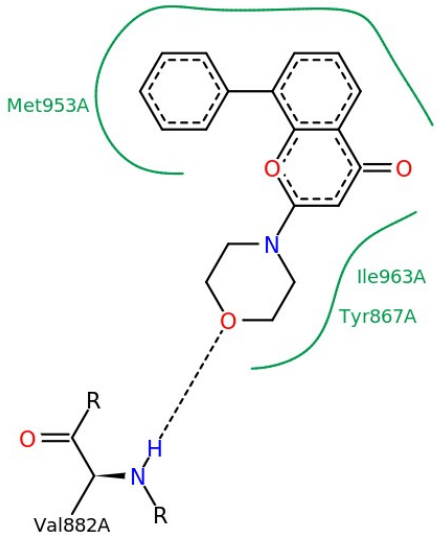 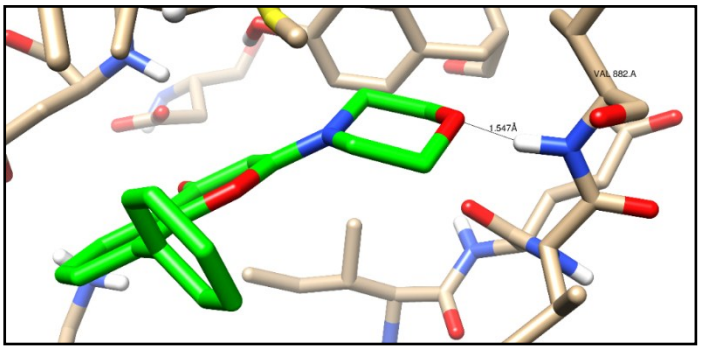					
Compound 2	**-13.38**	**H-acceptor**	**1.55**	**C=O**	**Val 882**

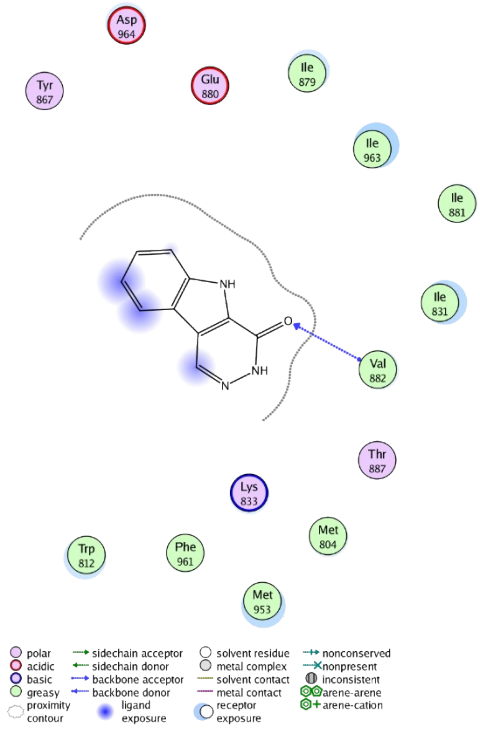

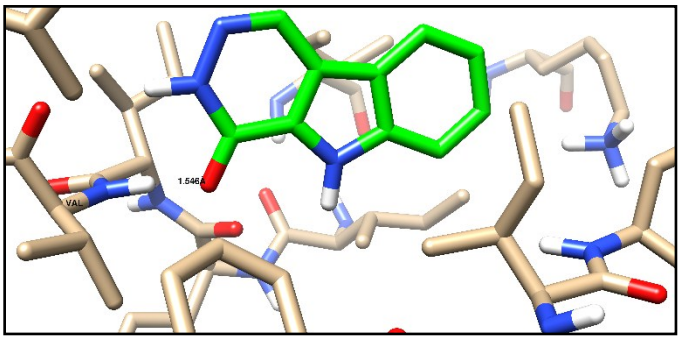

10	**-14.73**	**H-acceptor**	**1.68**	**-N-**	**NH -Val 882**

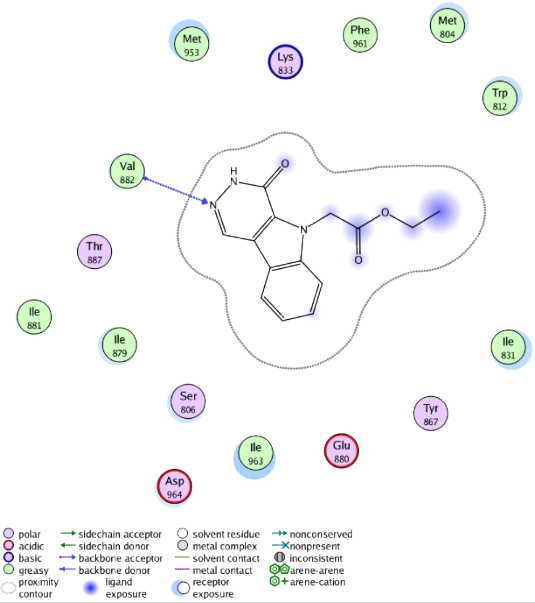

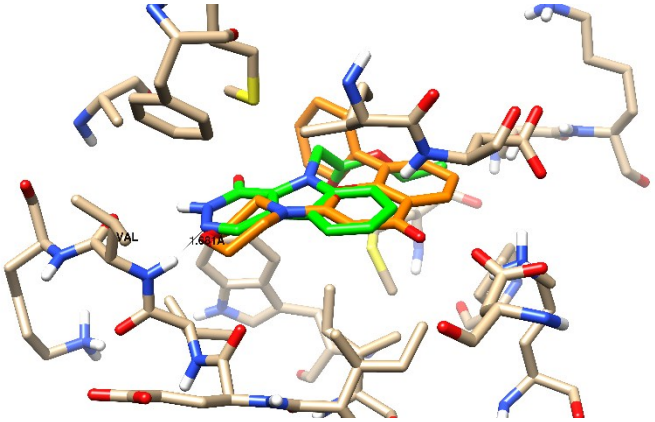

11	**-10.6**	**H-acceptor**	**1.65**	**C=O**	**NH -Val 882**

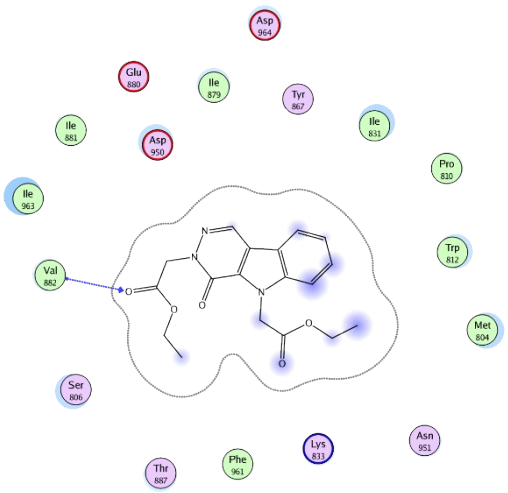

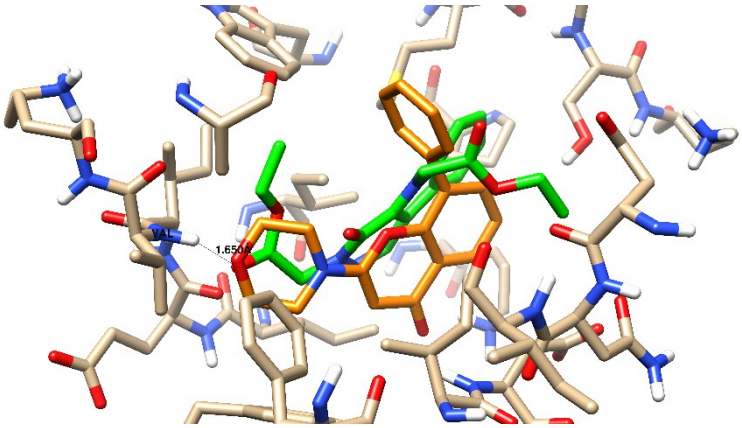

12	**-18.87**	**H-donor**	**2.06**	**N-H**	**C=O Val 882**

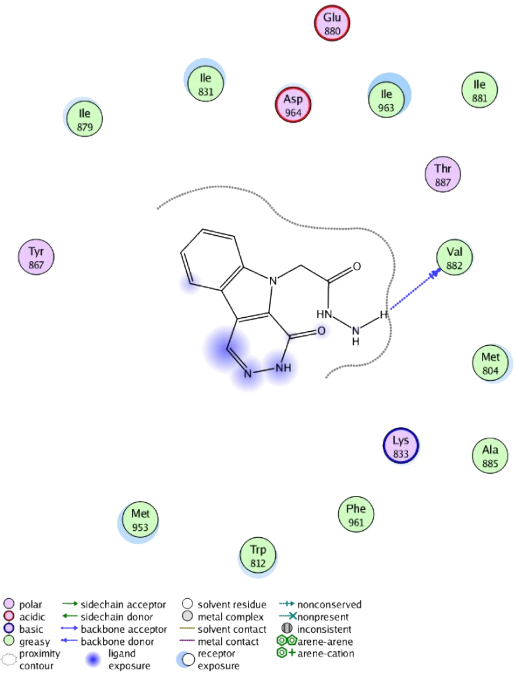

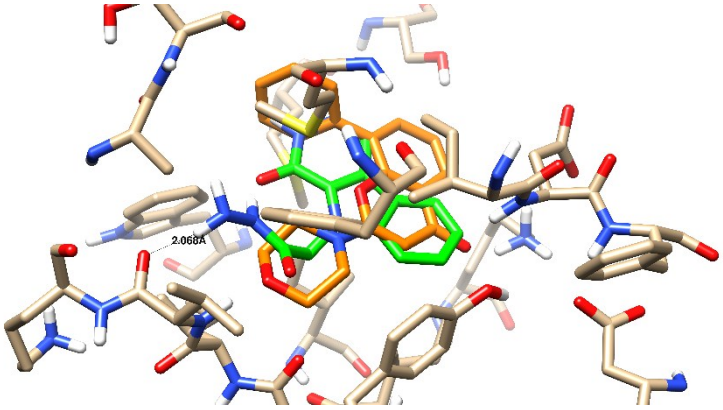

13	**-15.94**	H-donor H-acceptor	2.24 1.46	**NH** **C=O**	**Val 882** **Val 882**

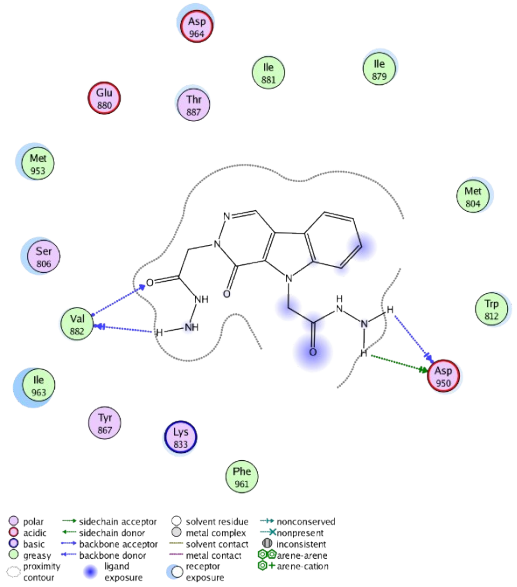

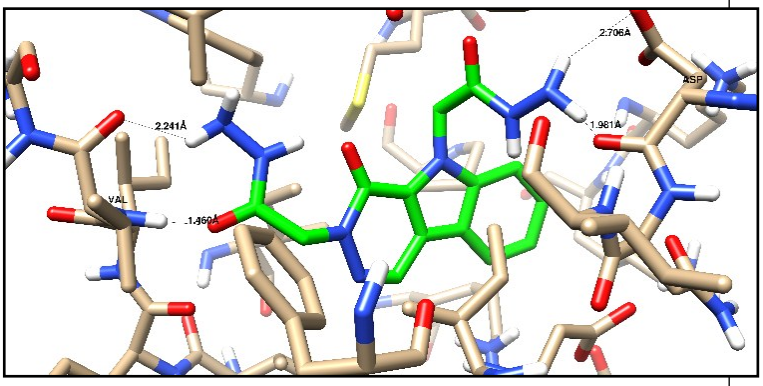

* Binding disposition and ligand-receptor interactions of Co-crystallized ligand (Orange) and docked compounds (green).

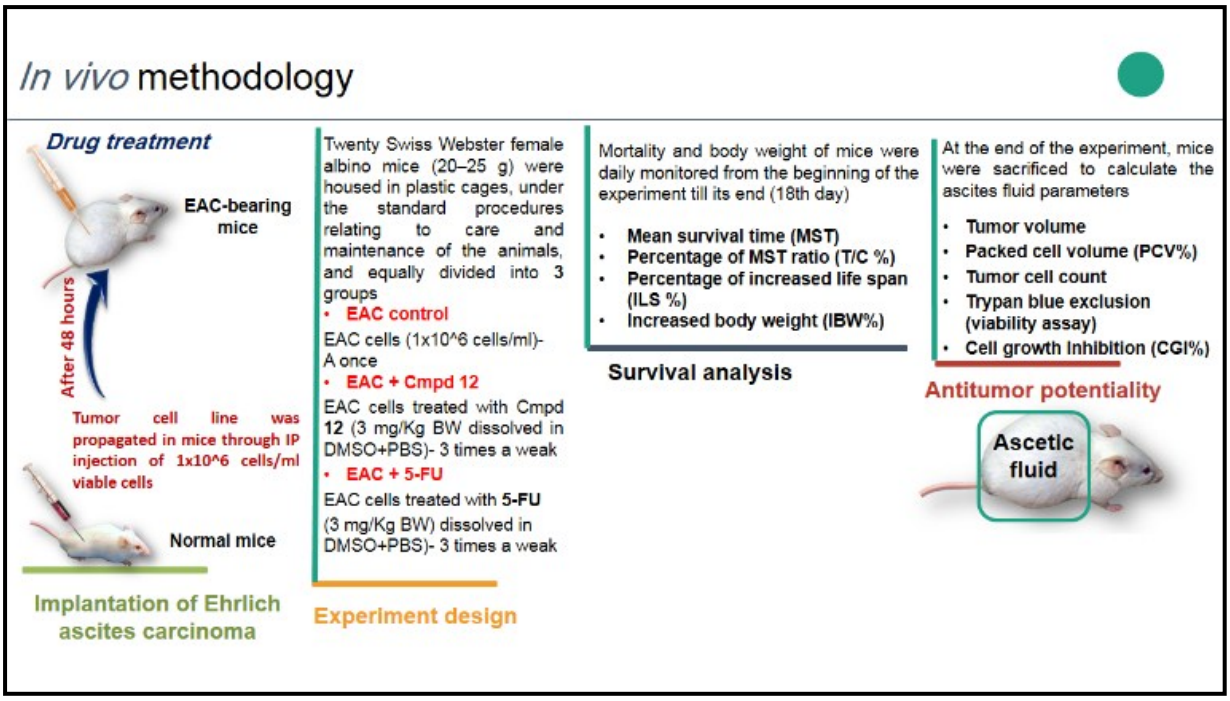

Supplementary image for the *in vivo* work (Fig. 6) (Nafie et al 2020)

NMR Spectra

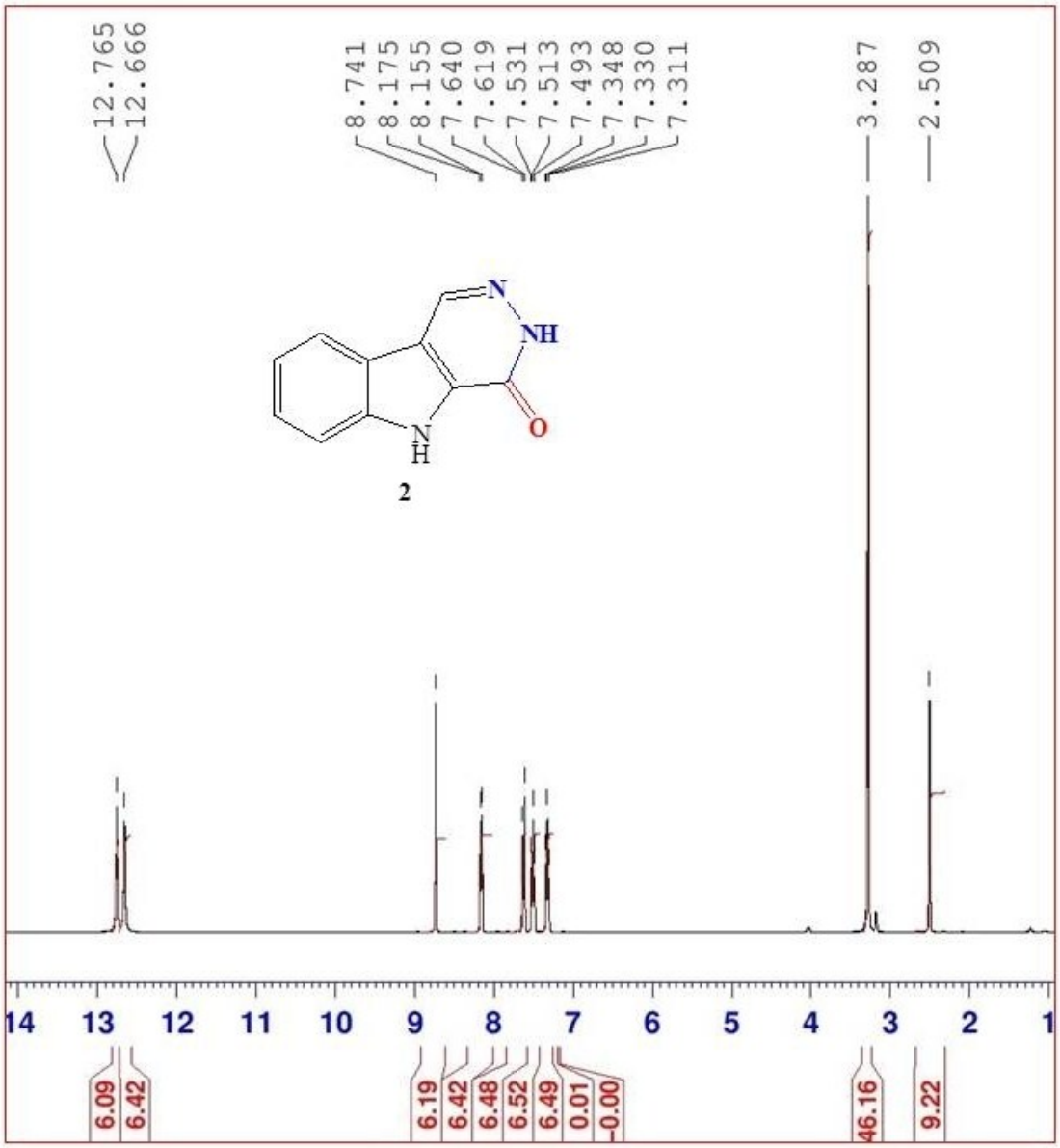

Figure S1: ^{1}HNMR of **2-** DMSO-d_6

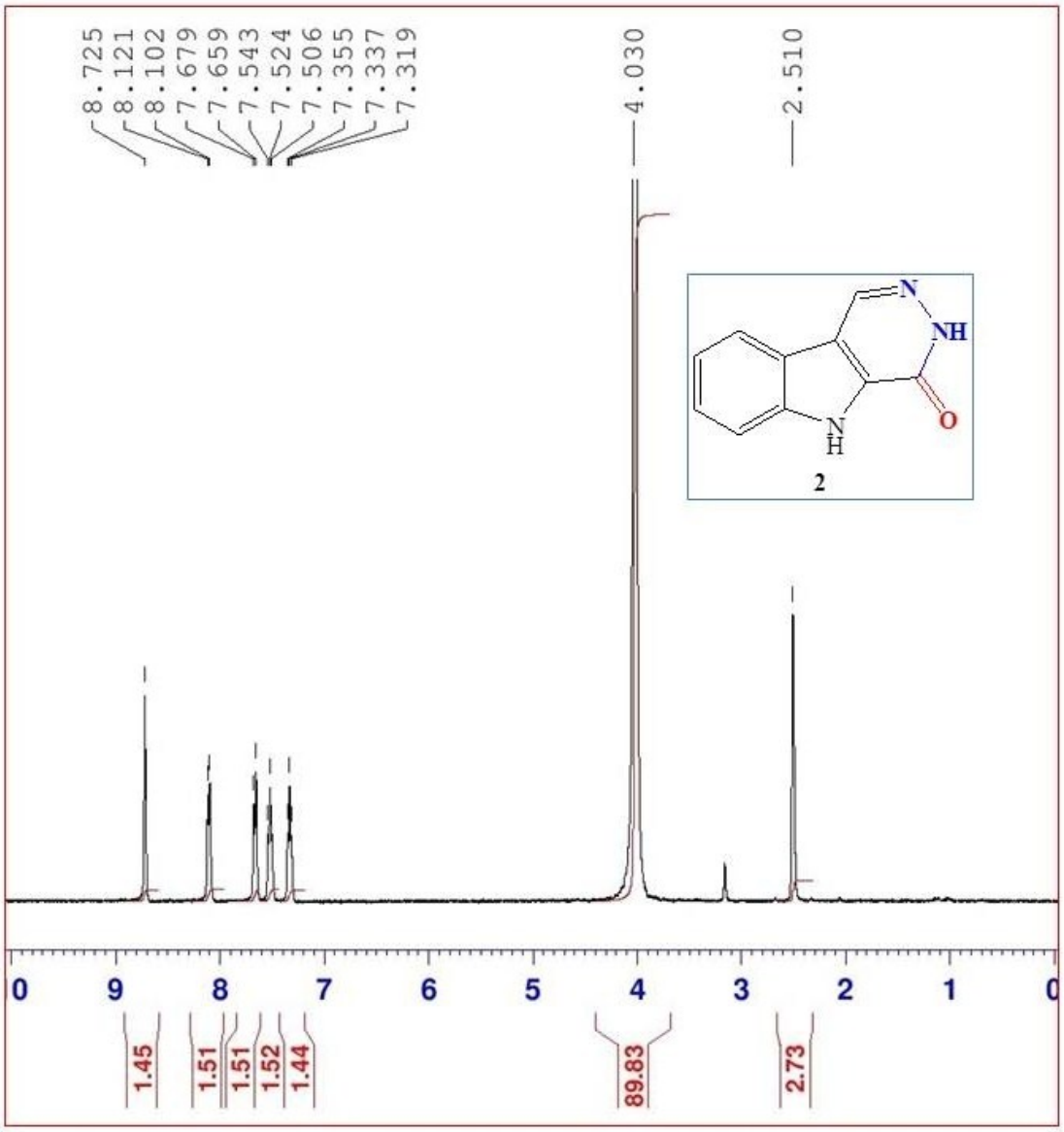

Figure S2: ^{1}H NMR of **2** in DMSO-d_6 + D_2O

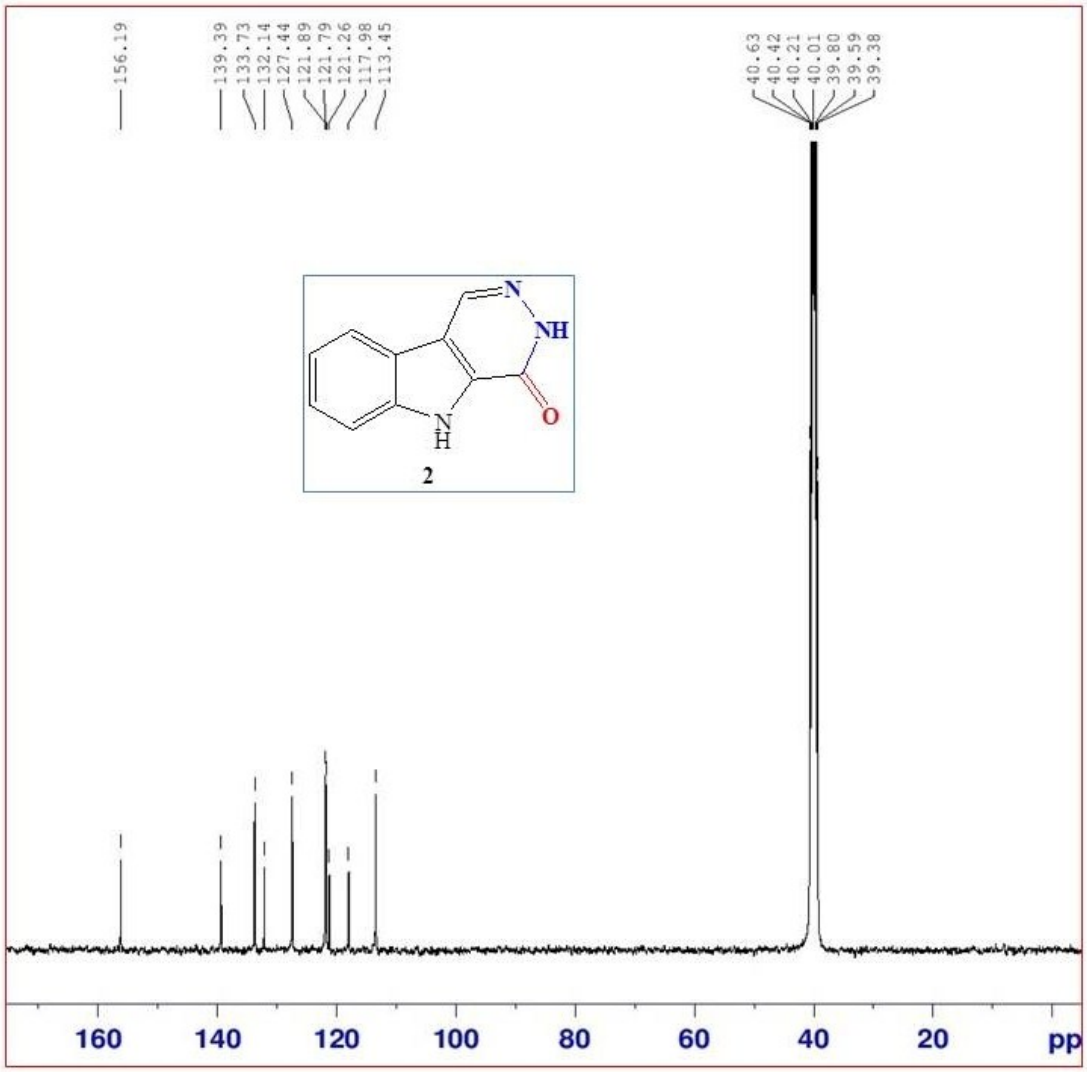

Figure S3: ^{13}CNMR of **2-** DMSO-d_6

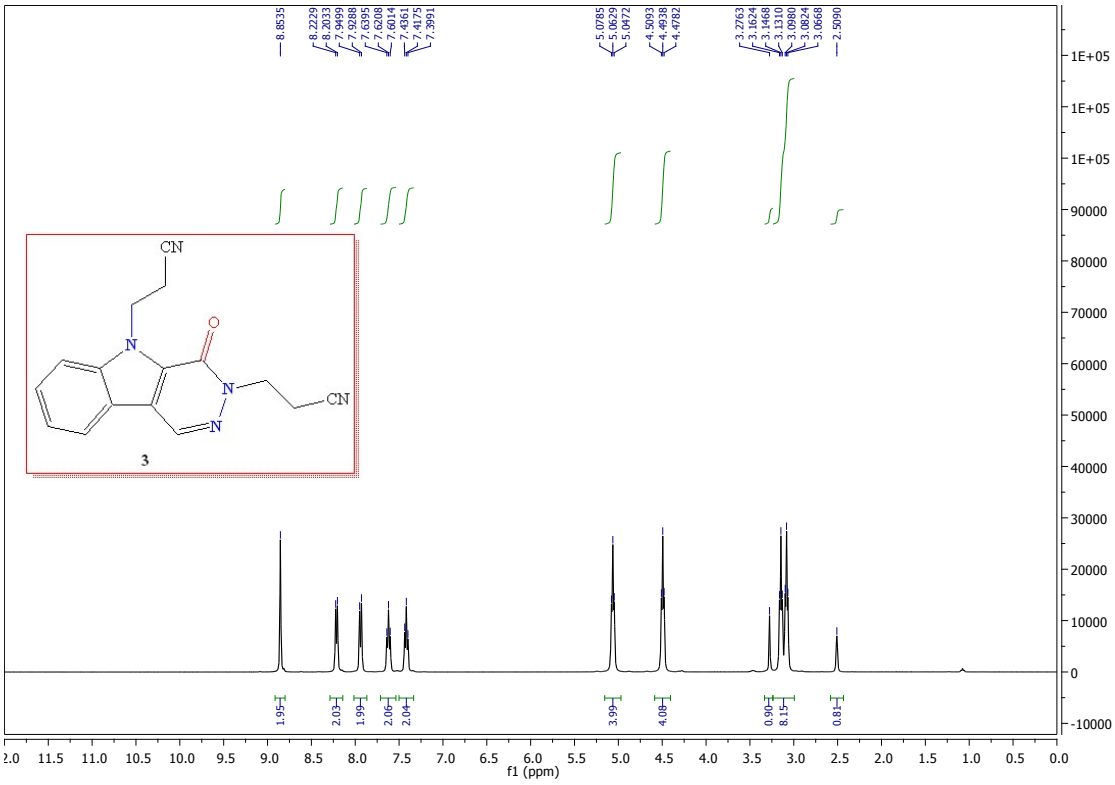

Figure S4: ^{1}HNMR of **3-** DMSO-d_6

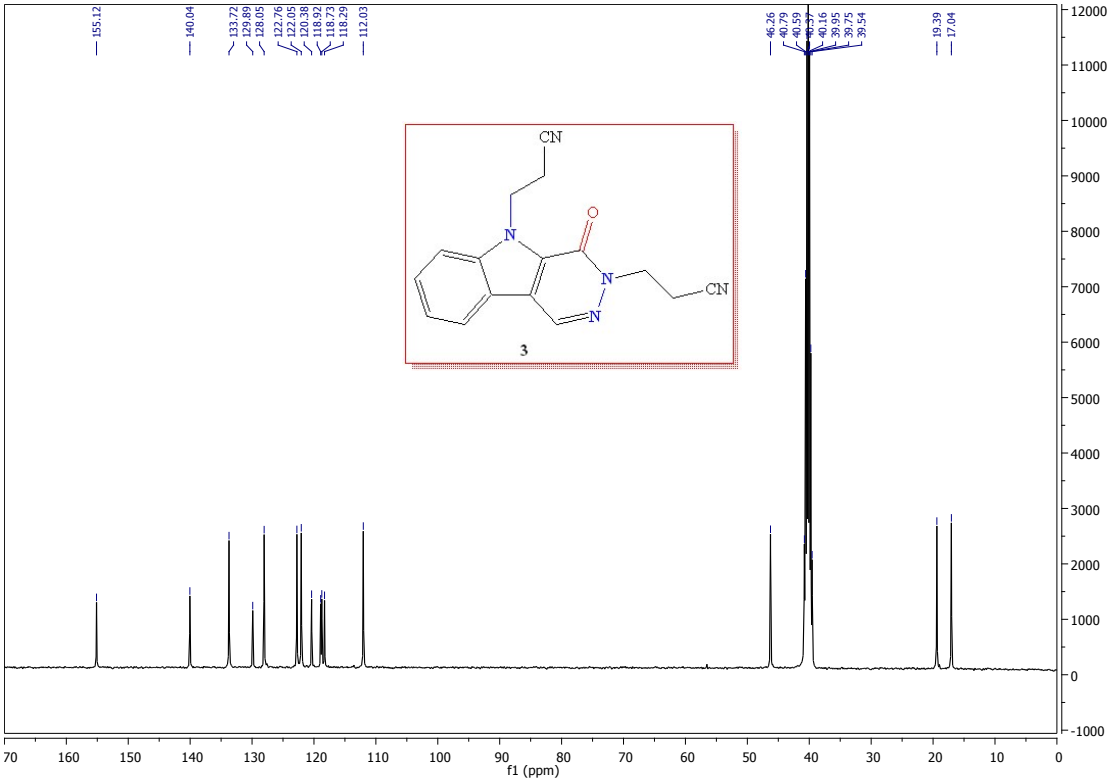

Figure S5: ^{13}CNMR of **3-** DMSO-d_6

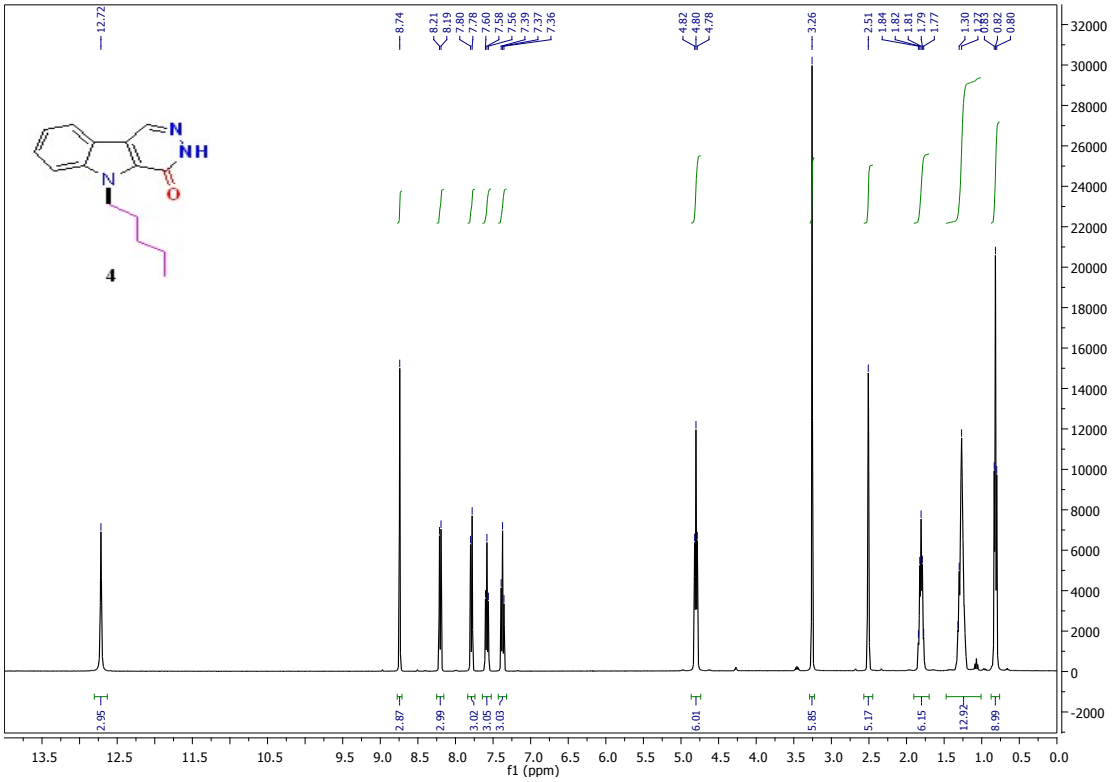

Figure S6: ^{1}HNMR of **4-** DMSO-d_6

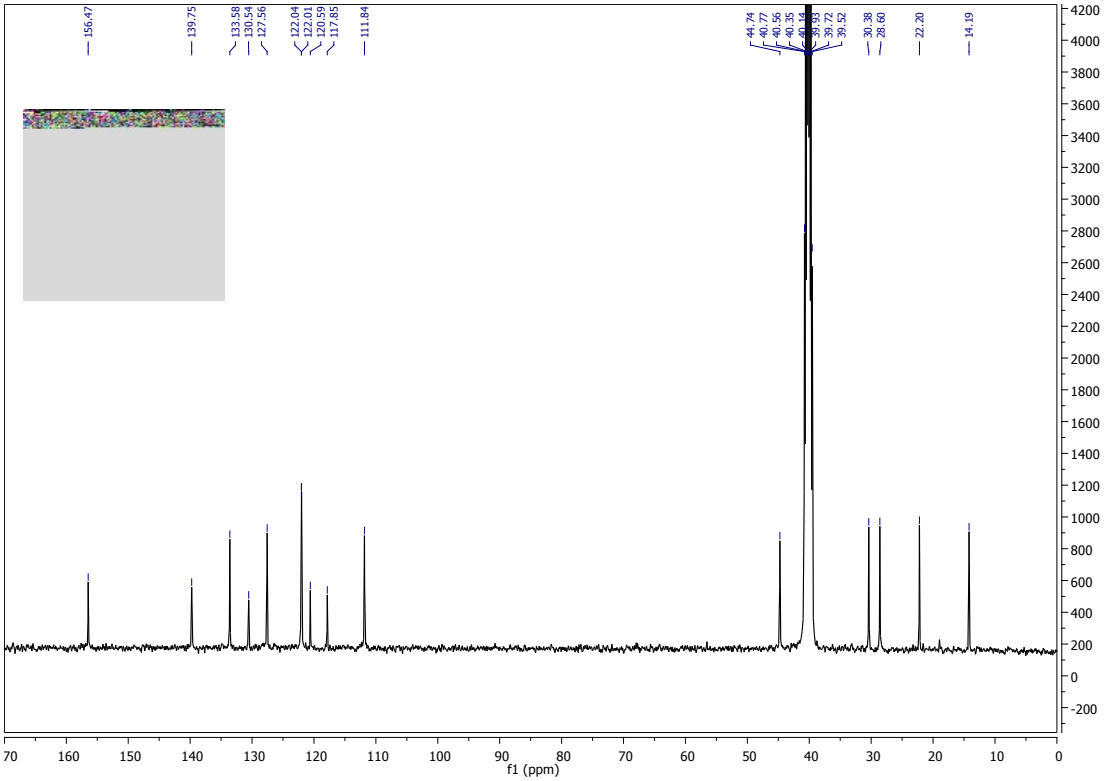

Figure S7: ^{13}CNMR of **4-** DMSO-d_6

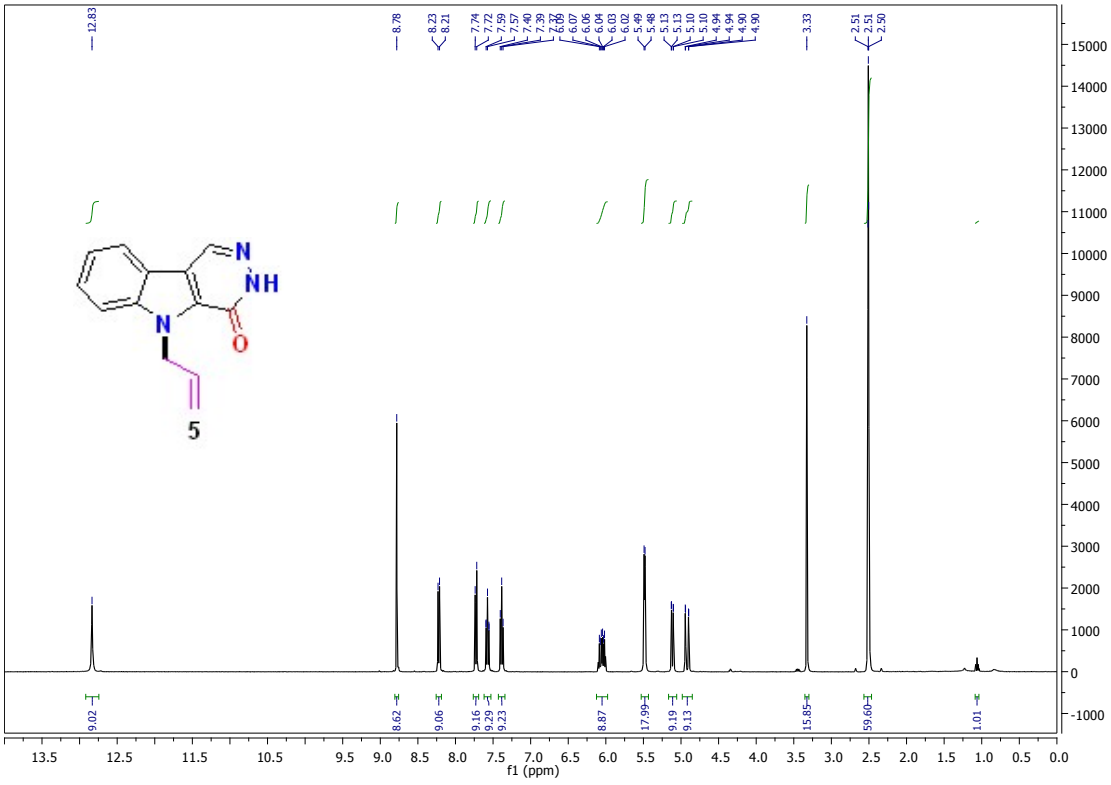

Figure S8: ^{1}HNMR of **5-** DMSO-d_6

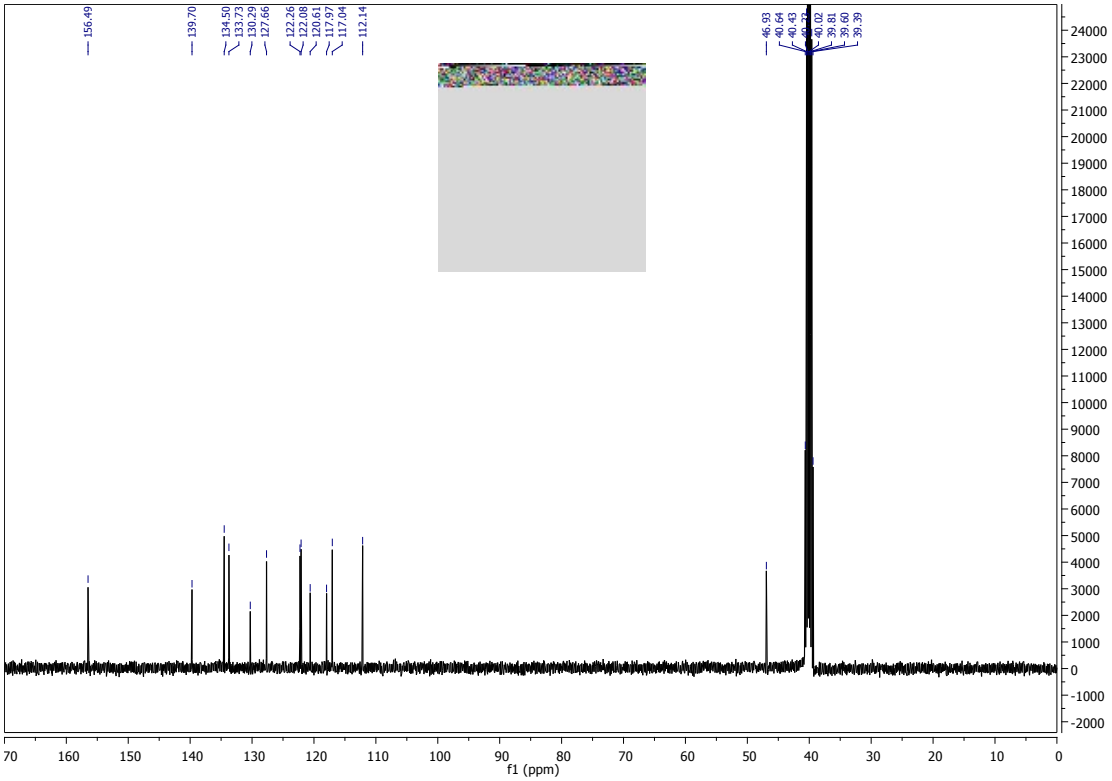

Figure S9: ^{13}CNMR of **5-** DMSO-d_6

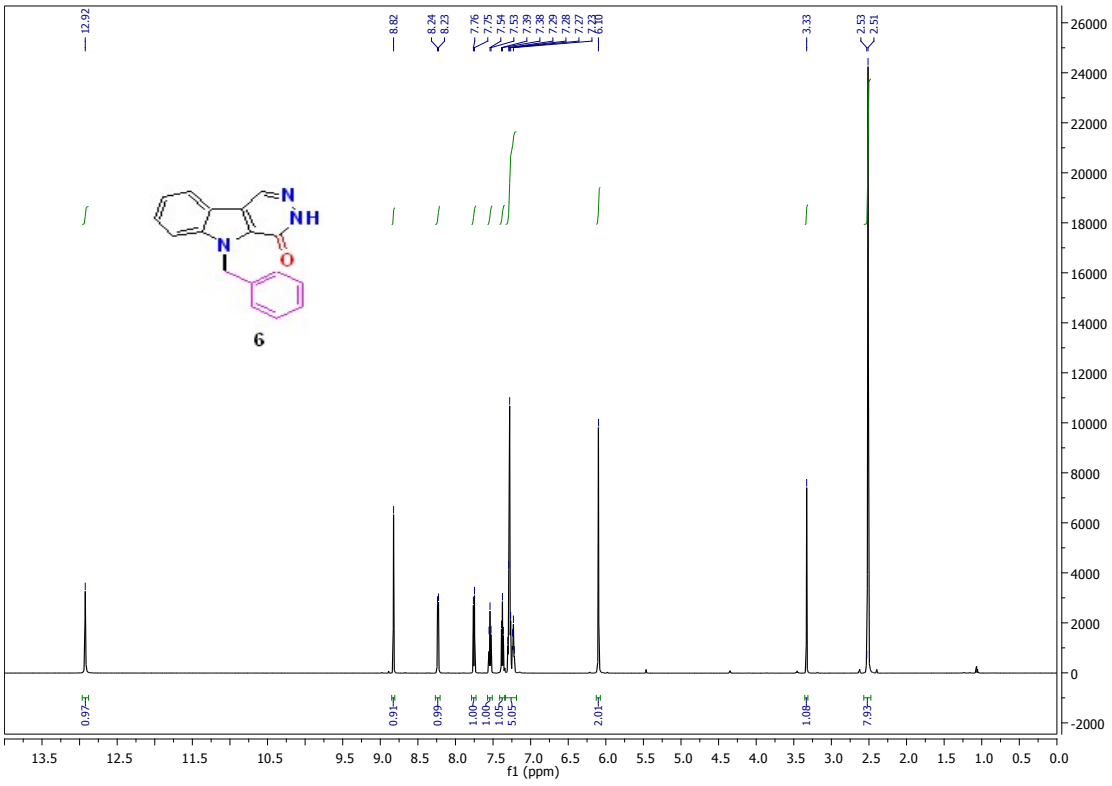

Figure S10: ^{1}HNMR of **6-** DMSO-d_6

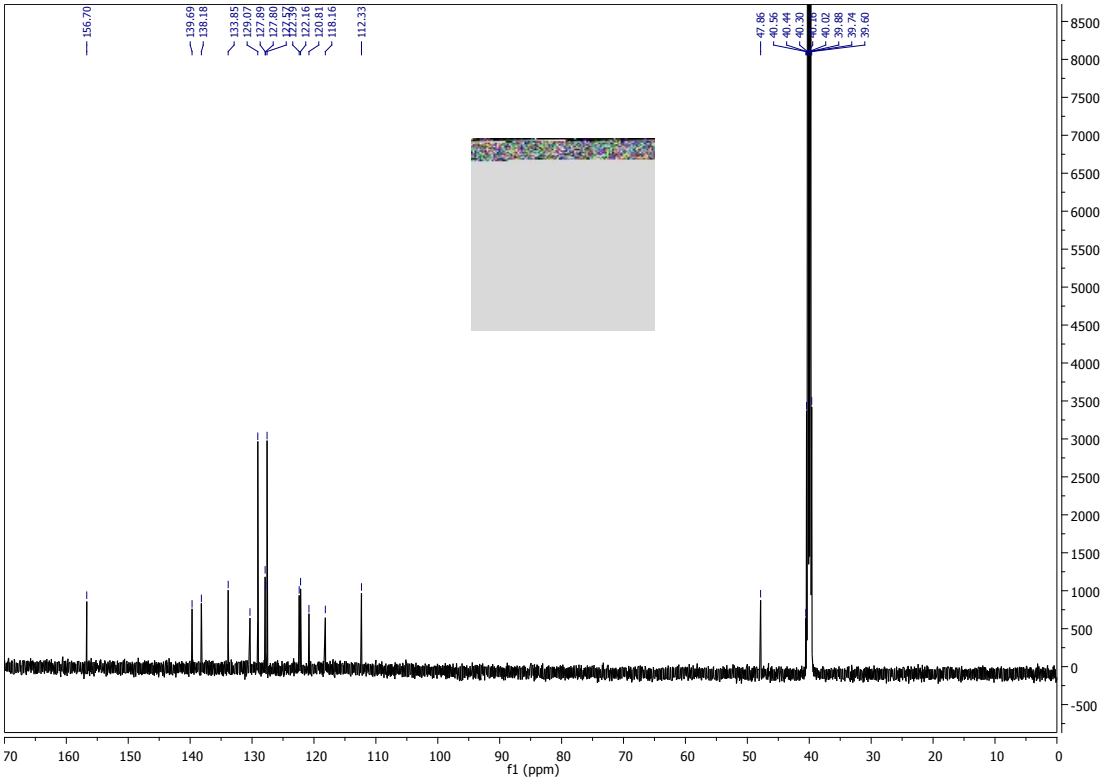

Figure S11: ^{13}CNMR of **6-** DMSO-d_6

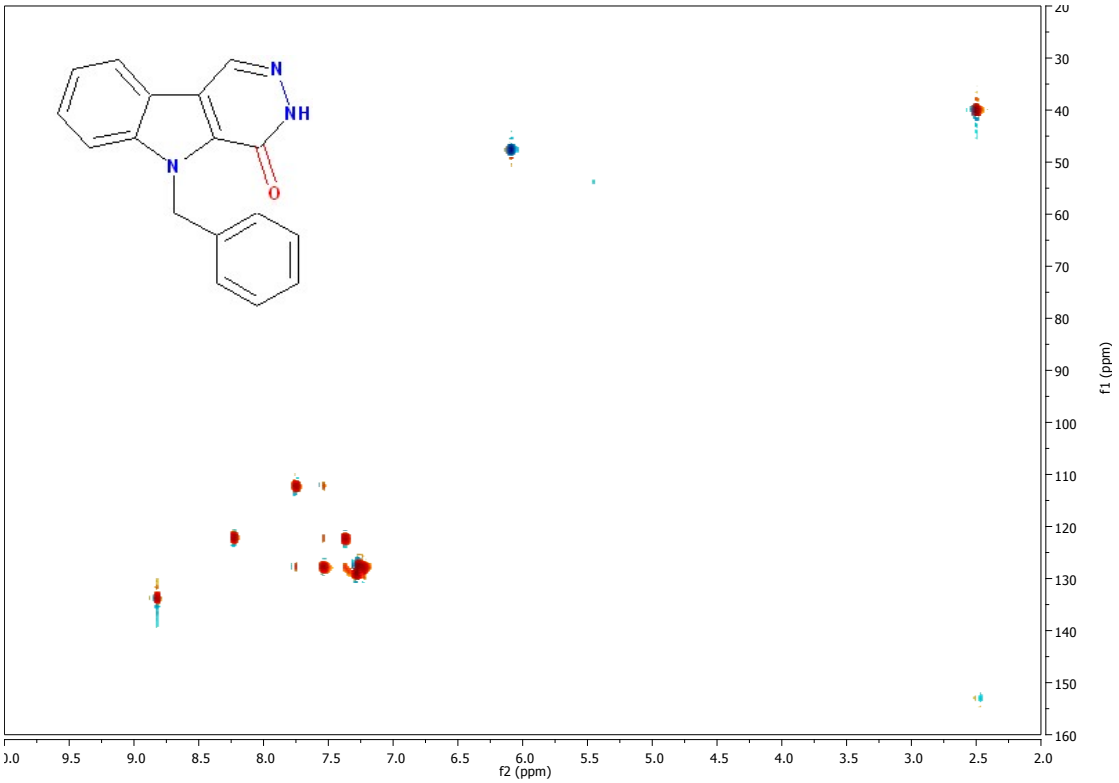

Figure S12: HMQC spectra of **6-** DMSO-d_6

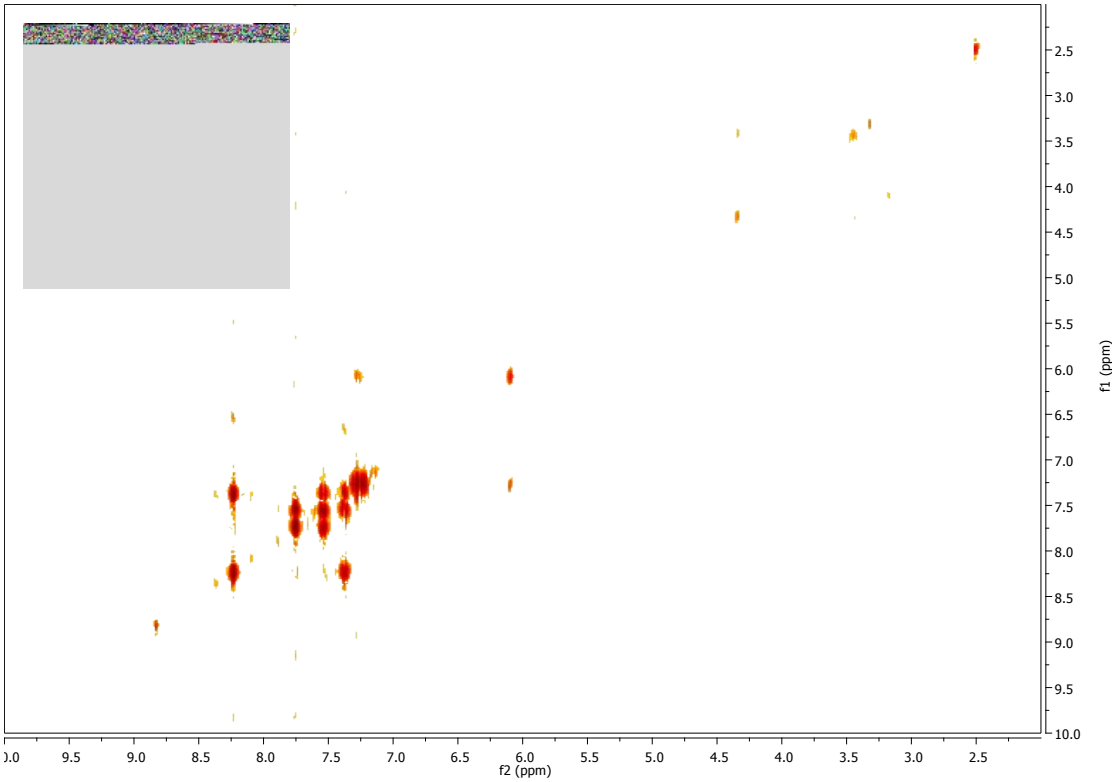

Figure S13: COSY spectra of **6-** DMSO-d_6

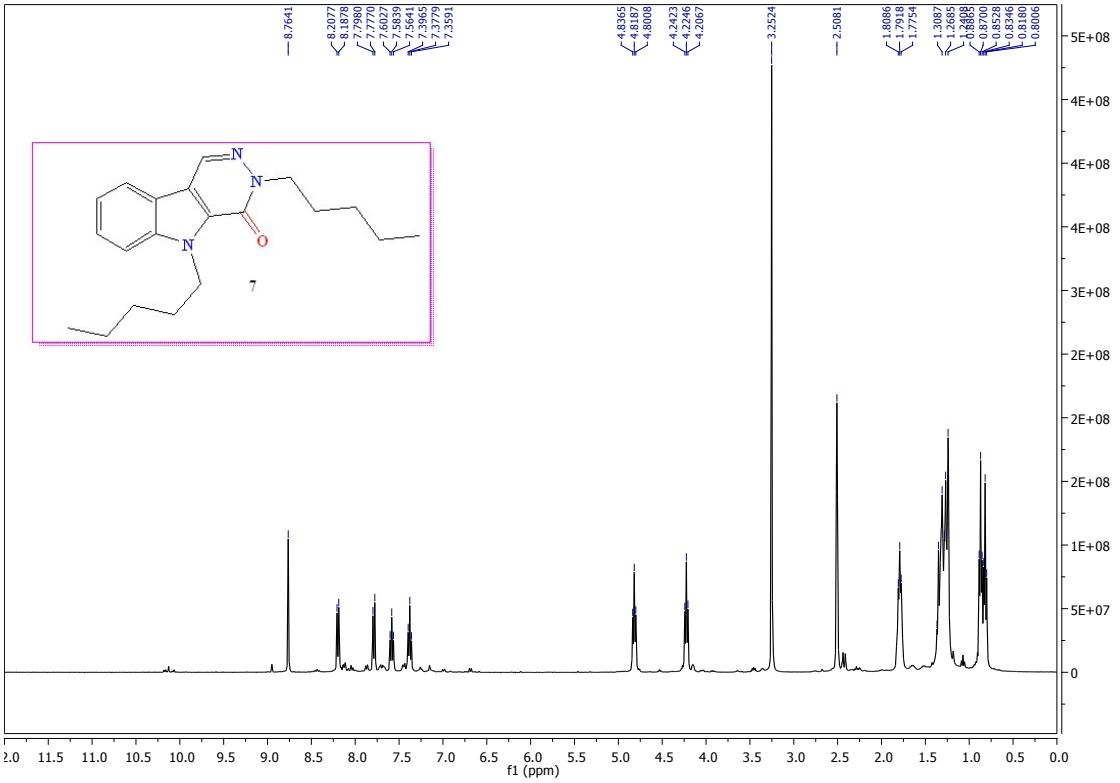

Figure S14: ^{1}HNMR of **7-** DMSO-d_6

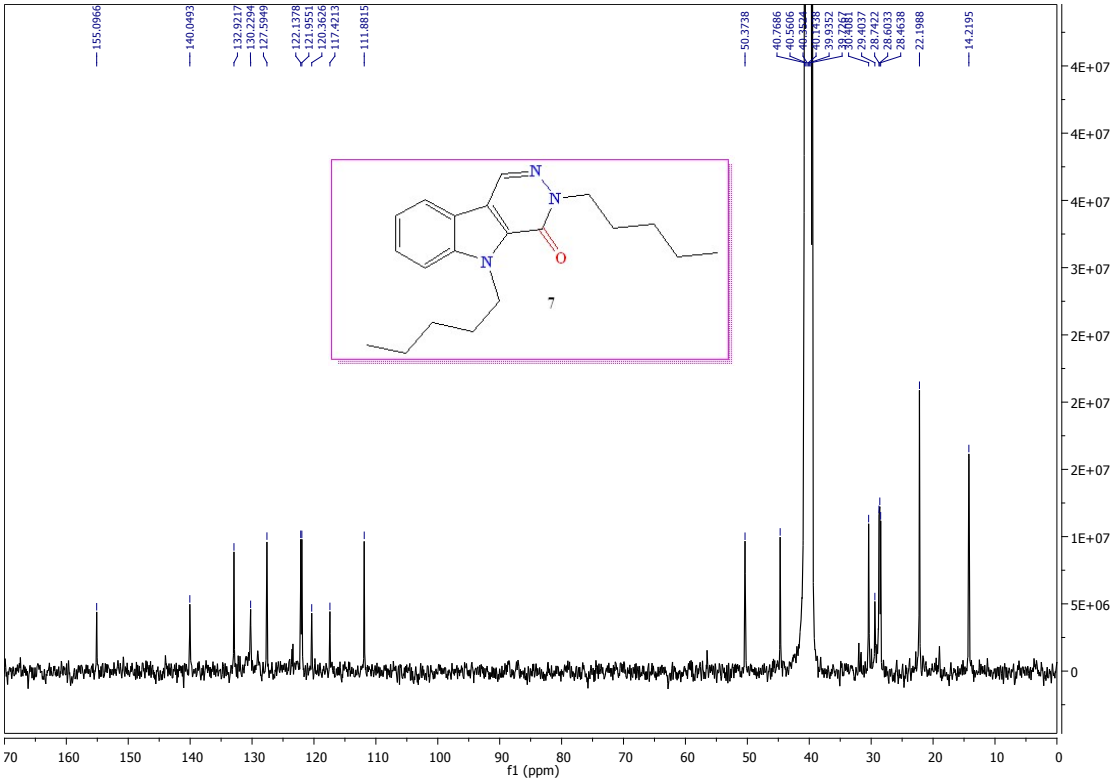

Figure S15: ^{13}CNMR of **7-** DMSO-d_6

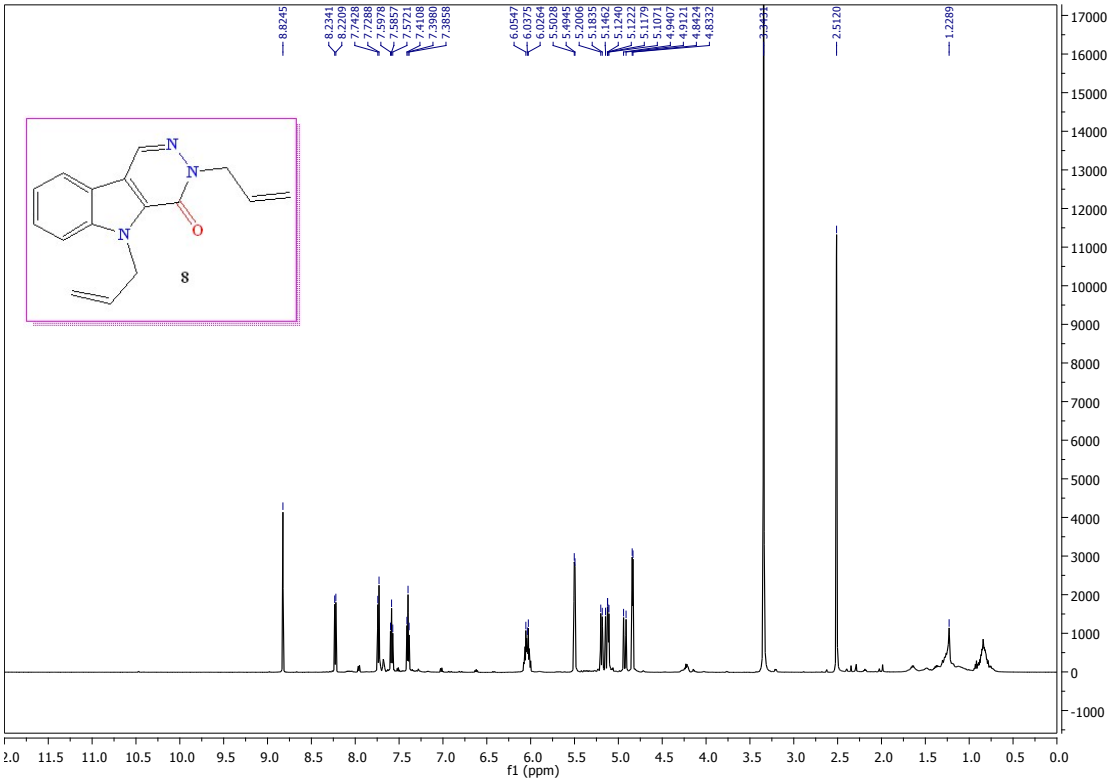

Figure S16: ^{1}HNMR of **8-** DMSO-d_6

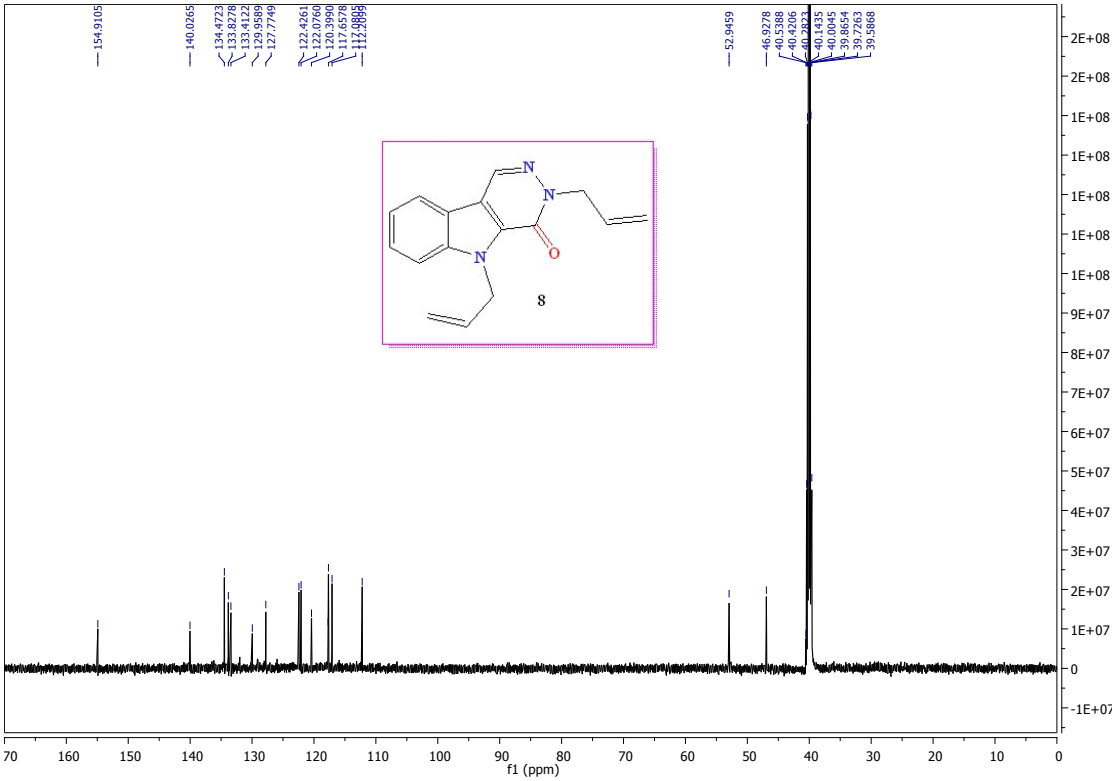

Figure S17: ^{13}CNMR of **8-** DMSO-d_6

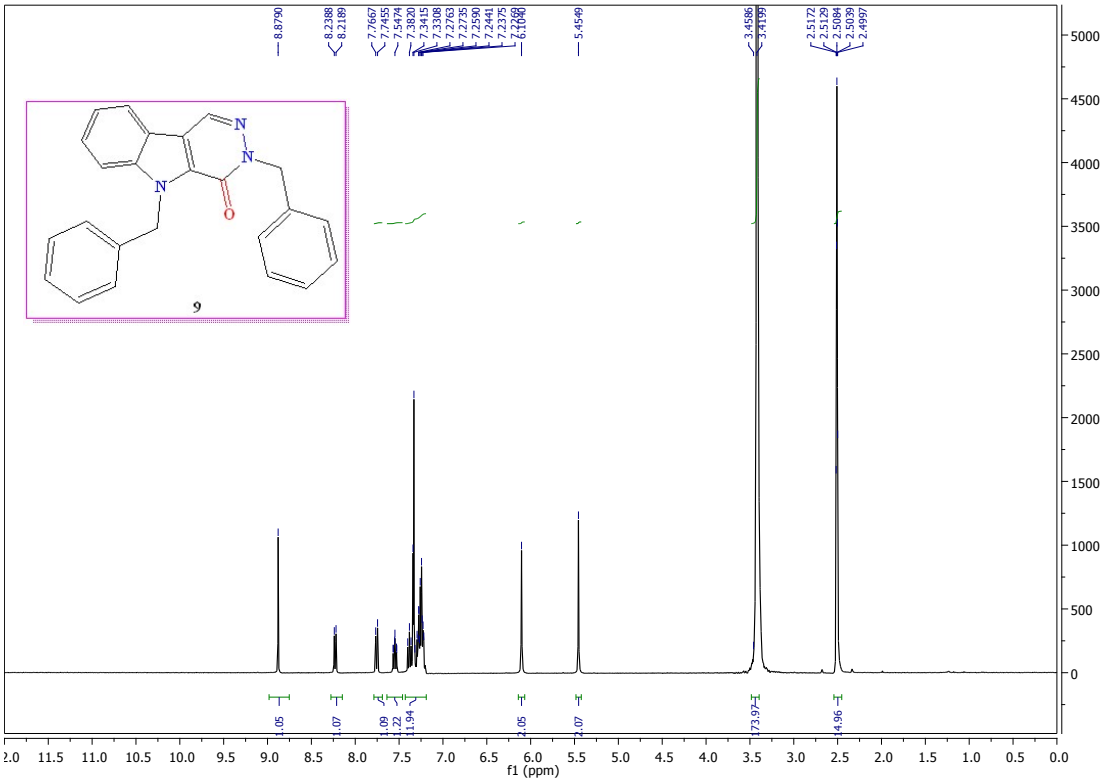

Figure S18: ^{1}HNMR of **9-** DMSO-d_6

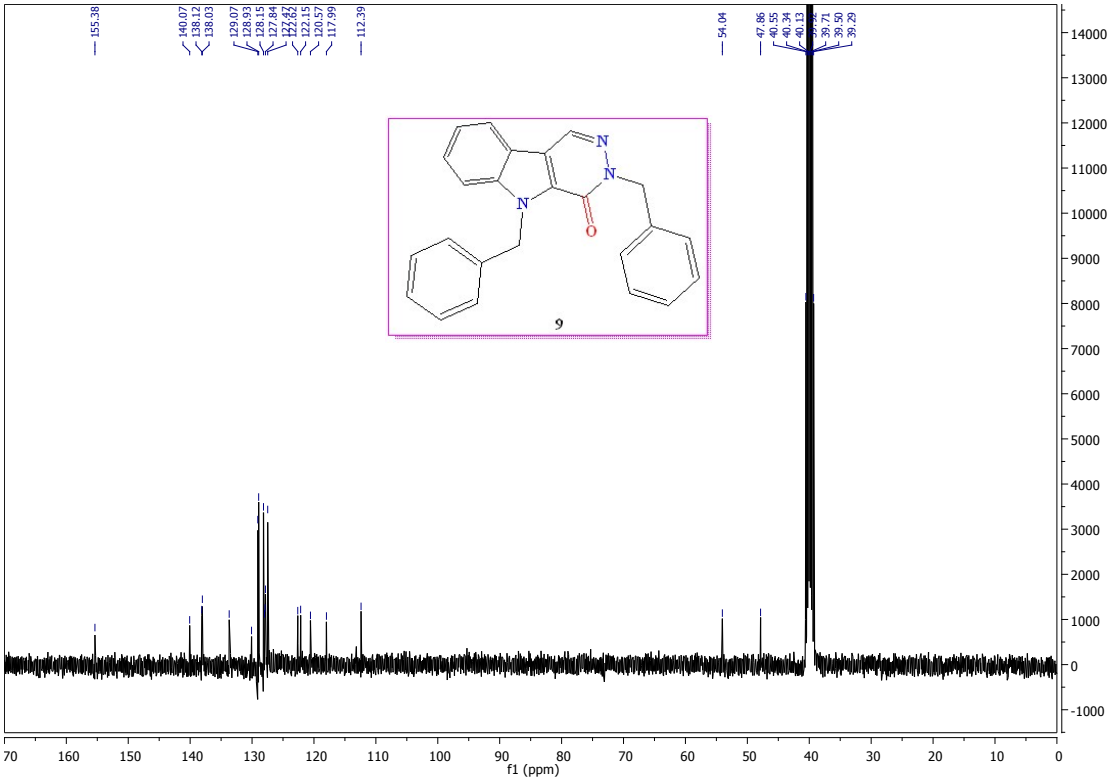

Figure S19: ^{13}CNMR of **9-** DMSO-d_6

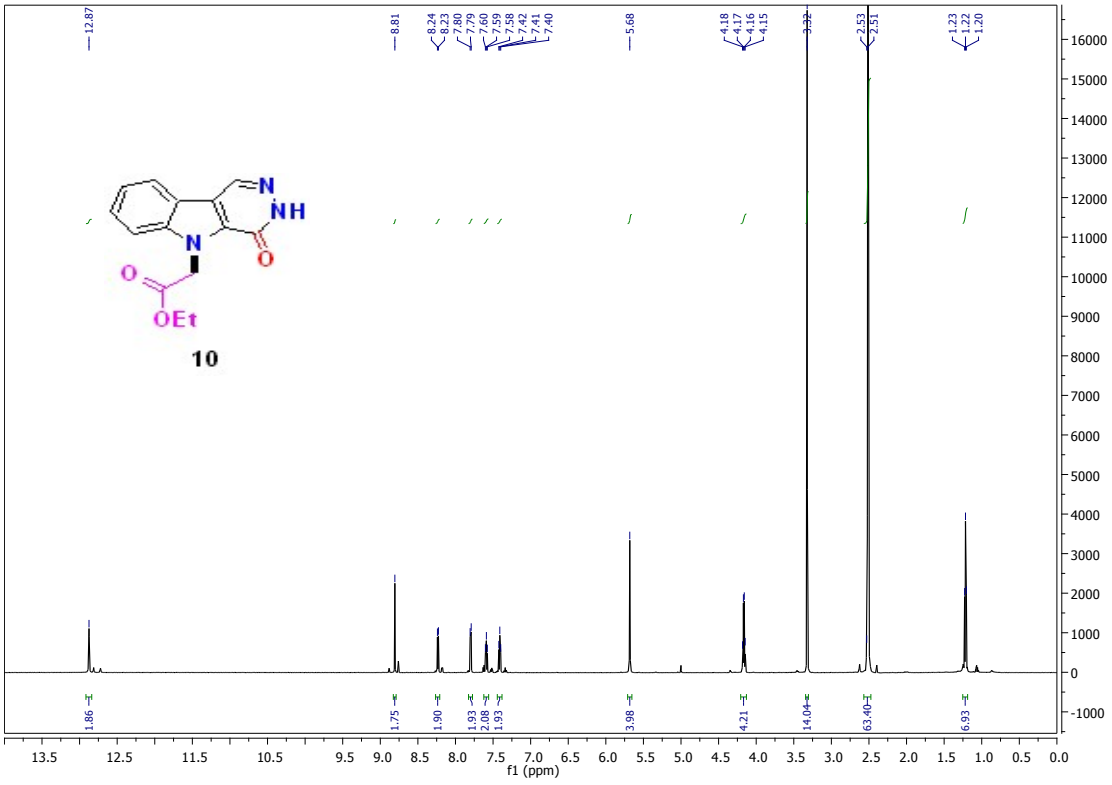

Figure S20: ^{1}HNMR of **10-** DMSO-d_6

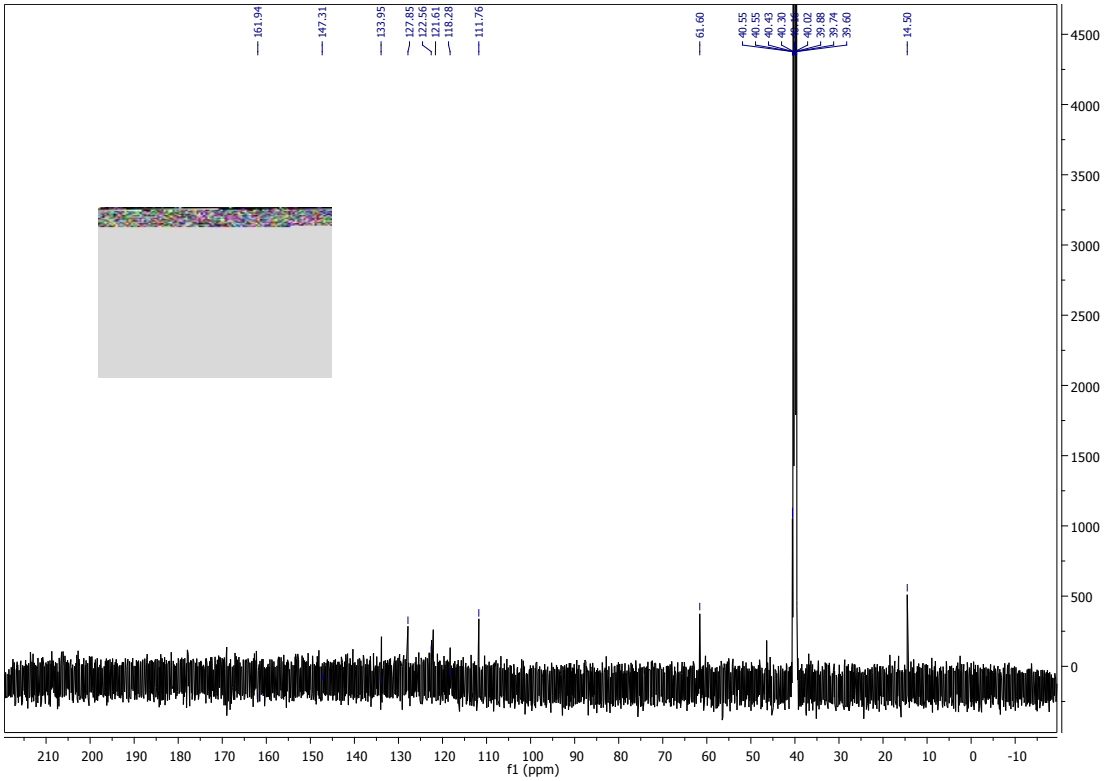

Figure S21: ^{13} CNMR of **10-** DMSO-d_6

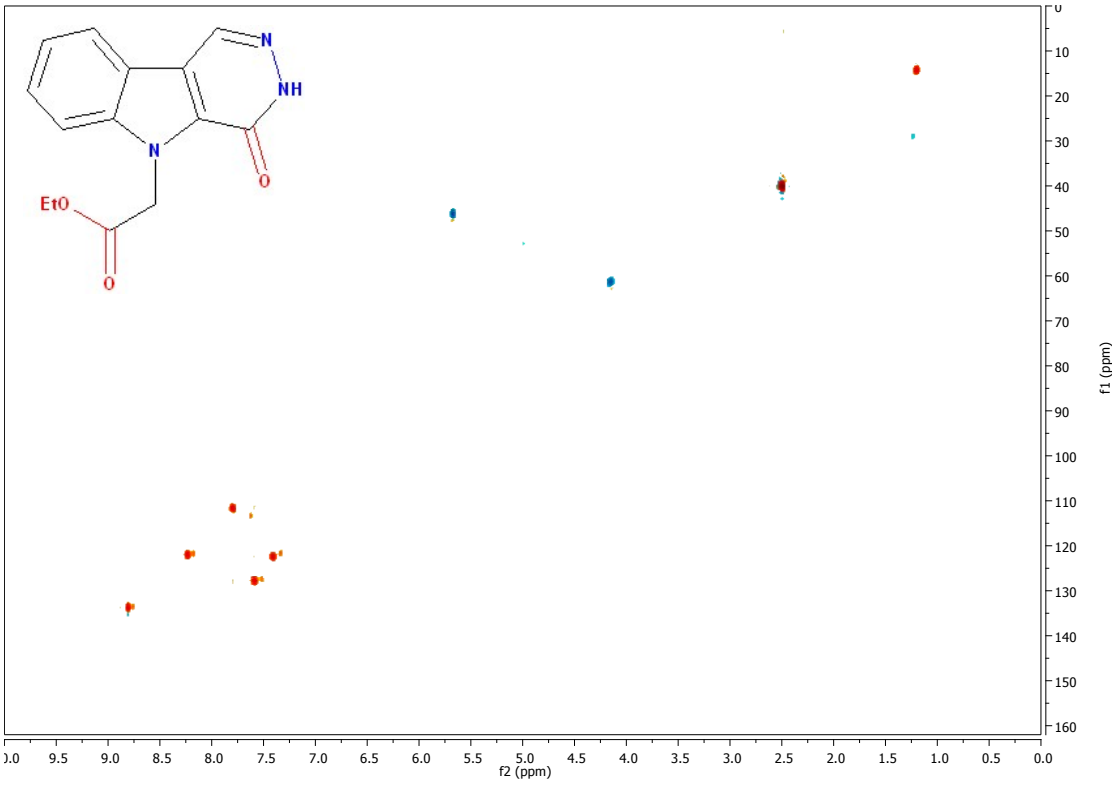

Figure S22: HMQC of **10-** DMSO-d_6

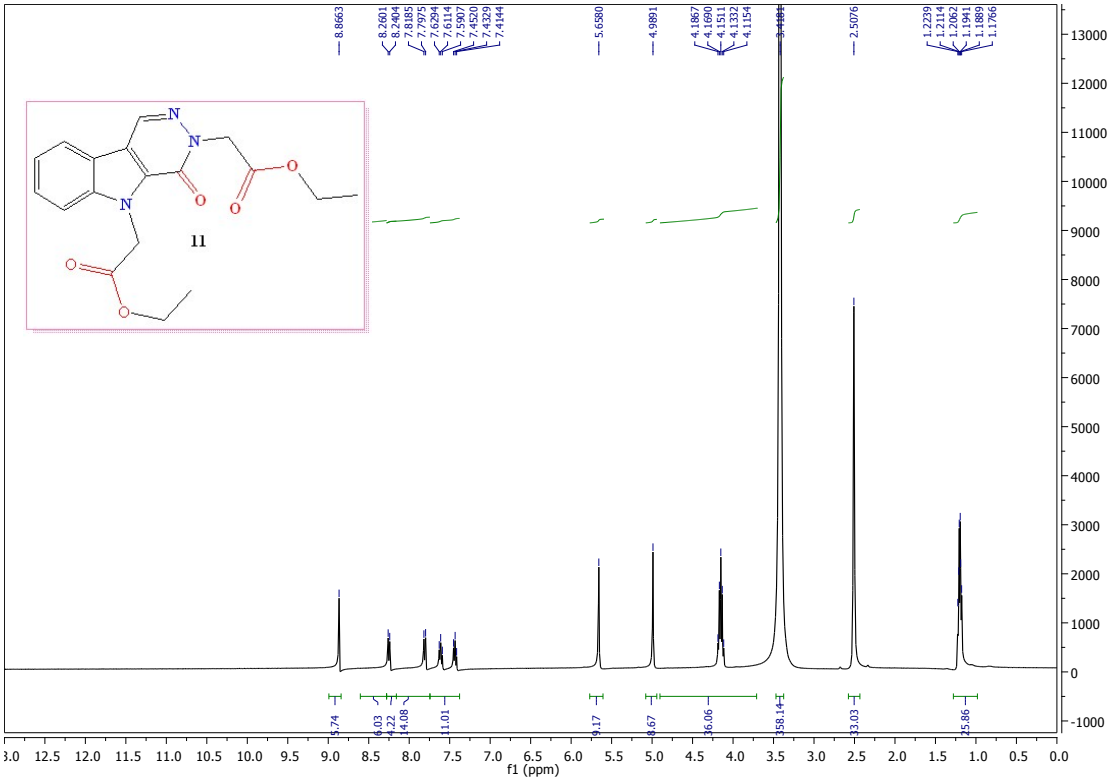

Figure S23: ^{1}HNMR of **11-** DMSO-d_6

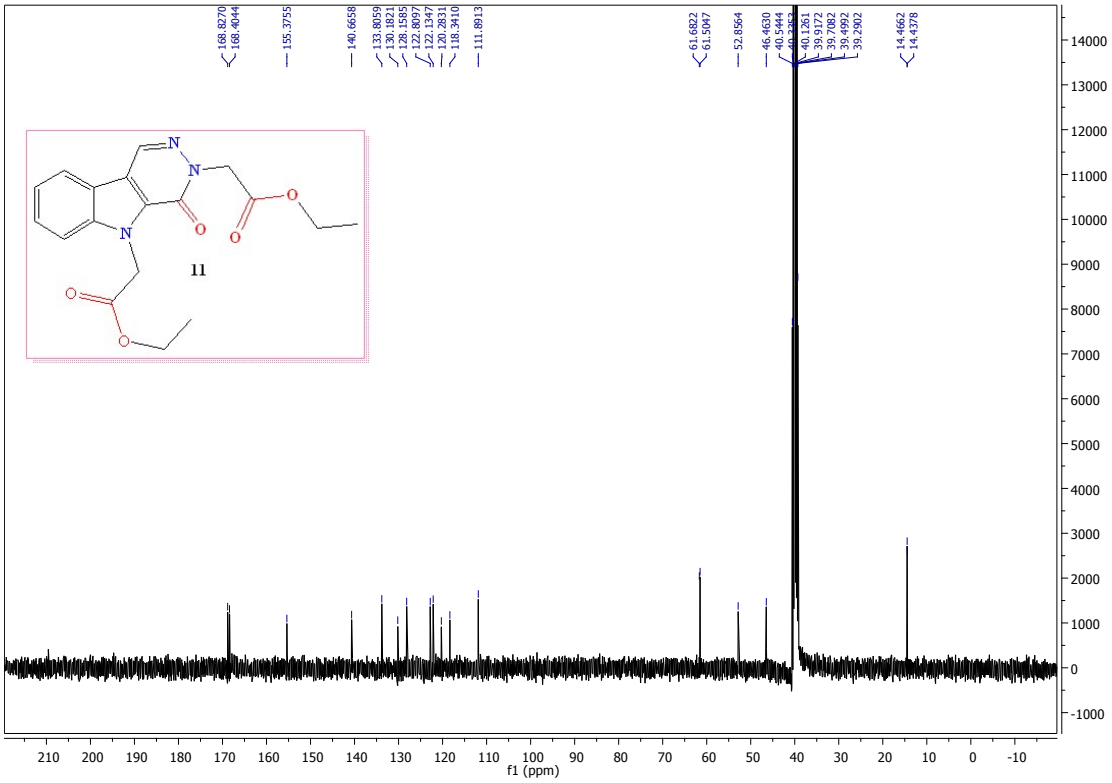

Figure S24: ^{13}CNMR of **11-** DMSO-d_6

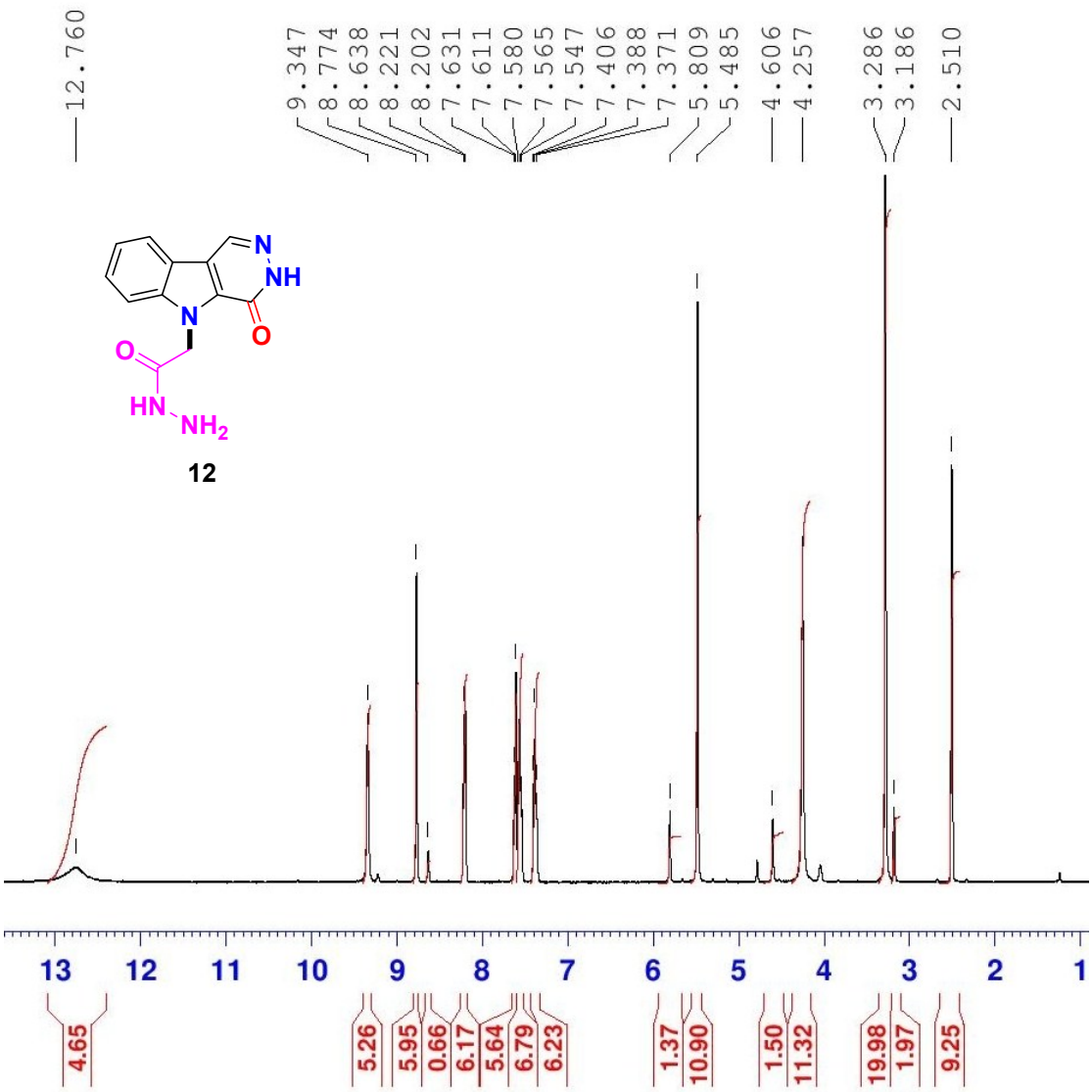

Figure S25: ^{1}HNMR of 1**2-** DMSO-d_6

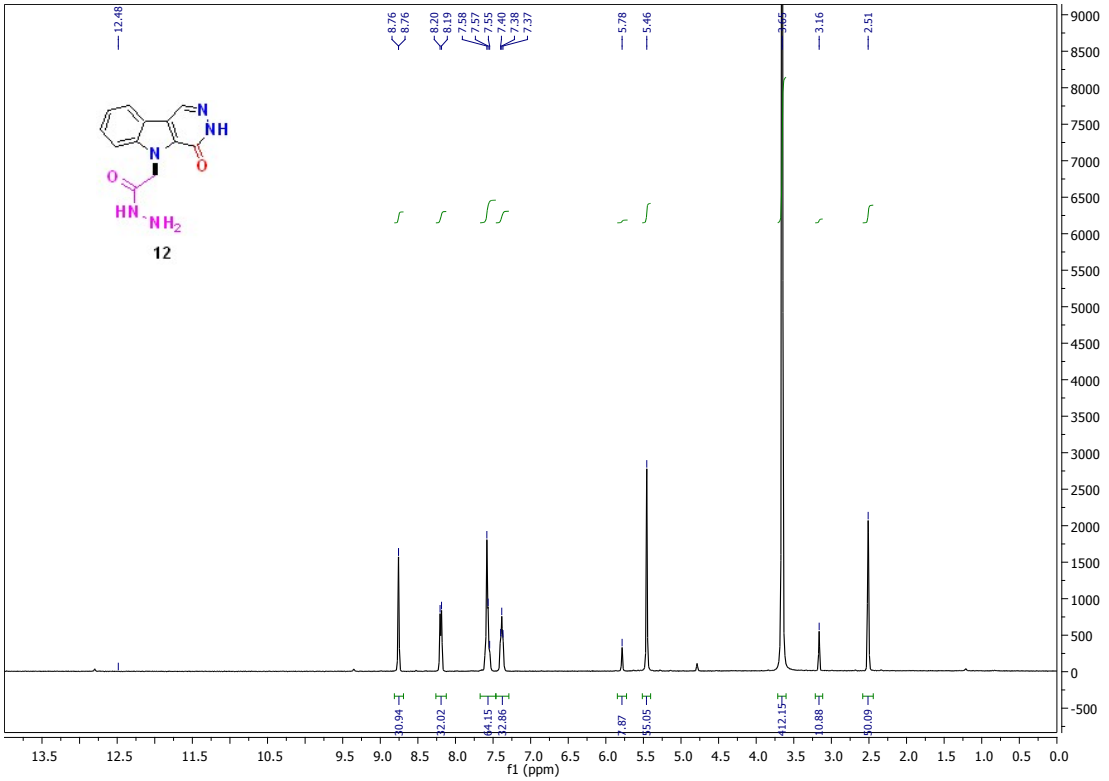

Figure S26: ^{1}HNMR of 1**2-** DMSO-d_6 + D_2O

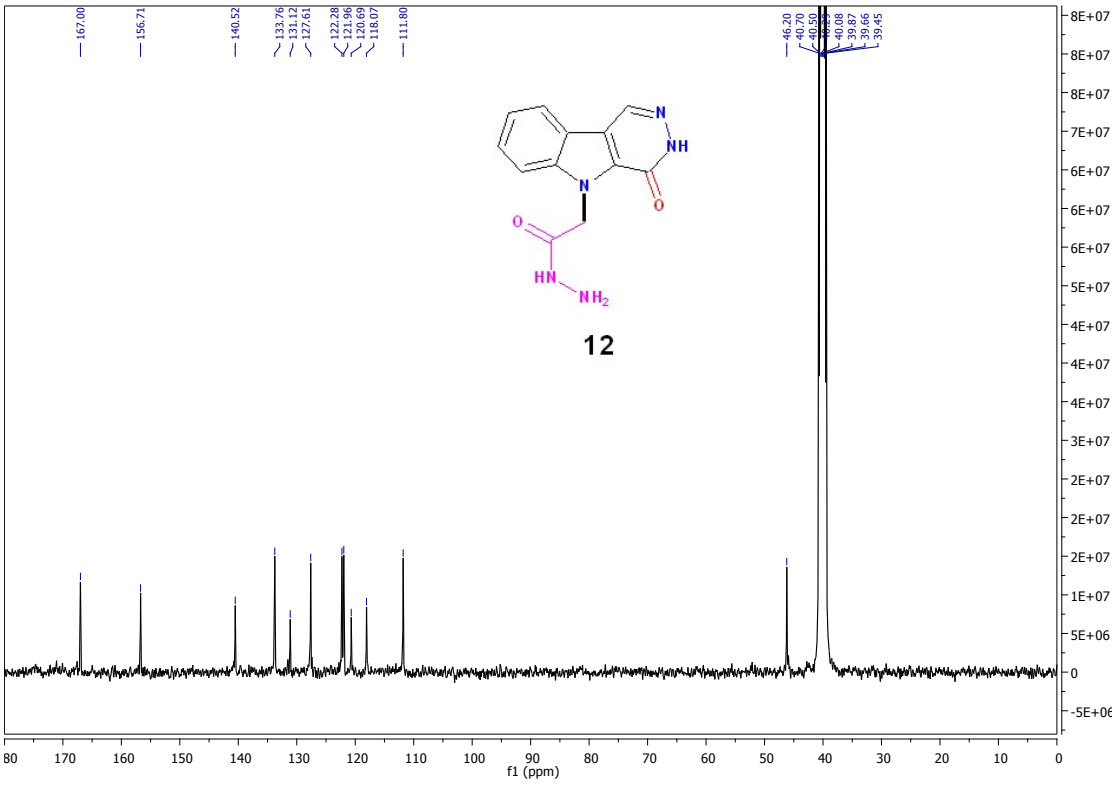

Figure S27: ^{13}CNMR of 1**2-** DMSO-d_6

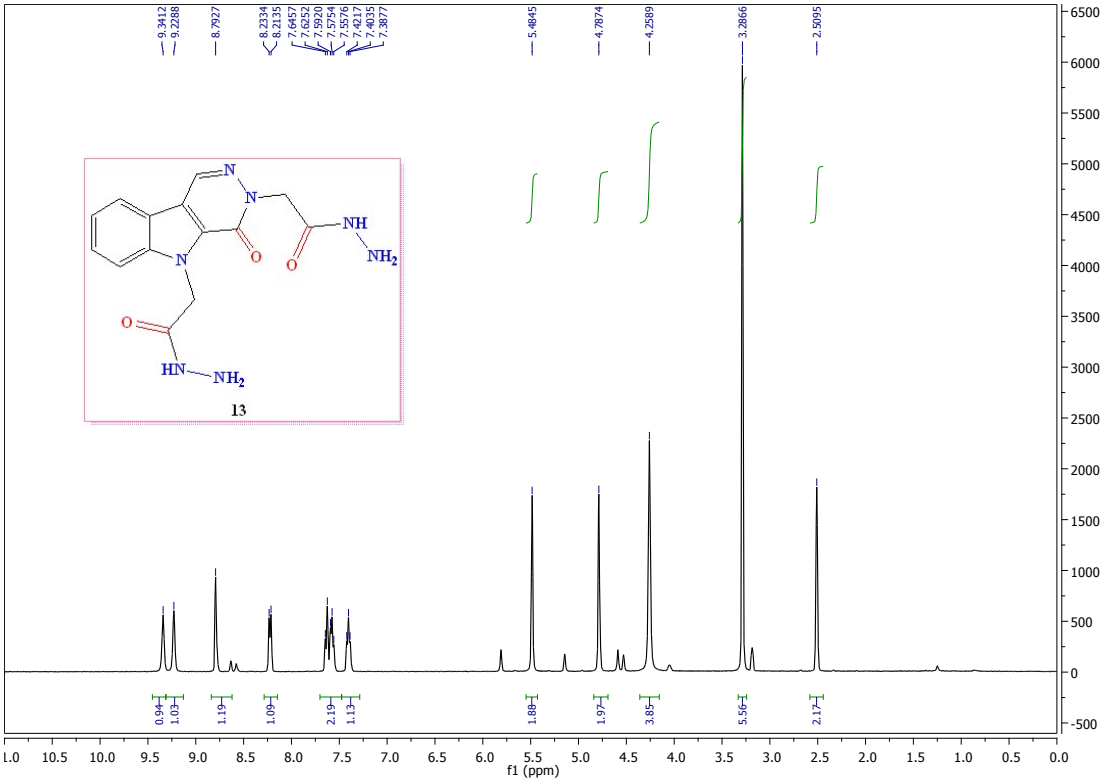

Figure S28: ^{1}HNMR of **13-** DMSO-d_6

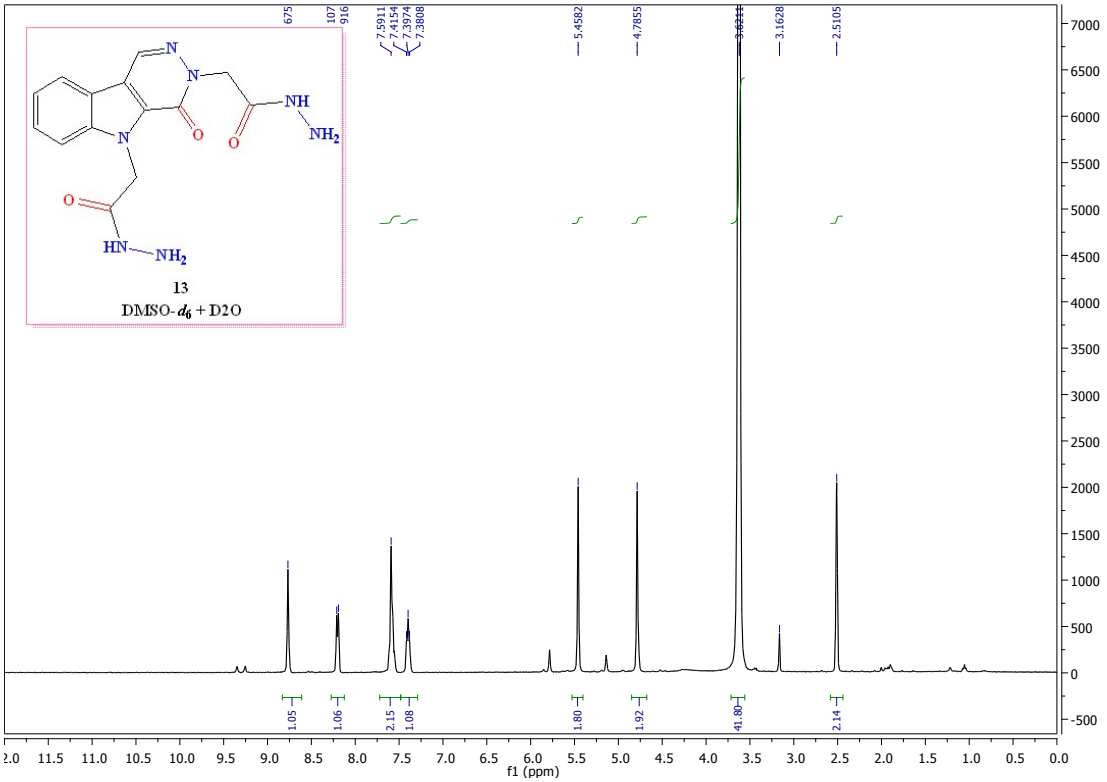

Figure S29: ^{1}HNMR of **13-** DMSO-d_6 + D_2O

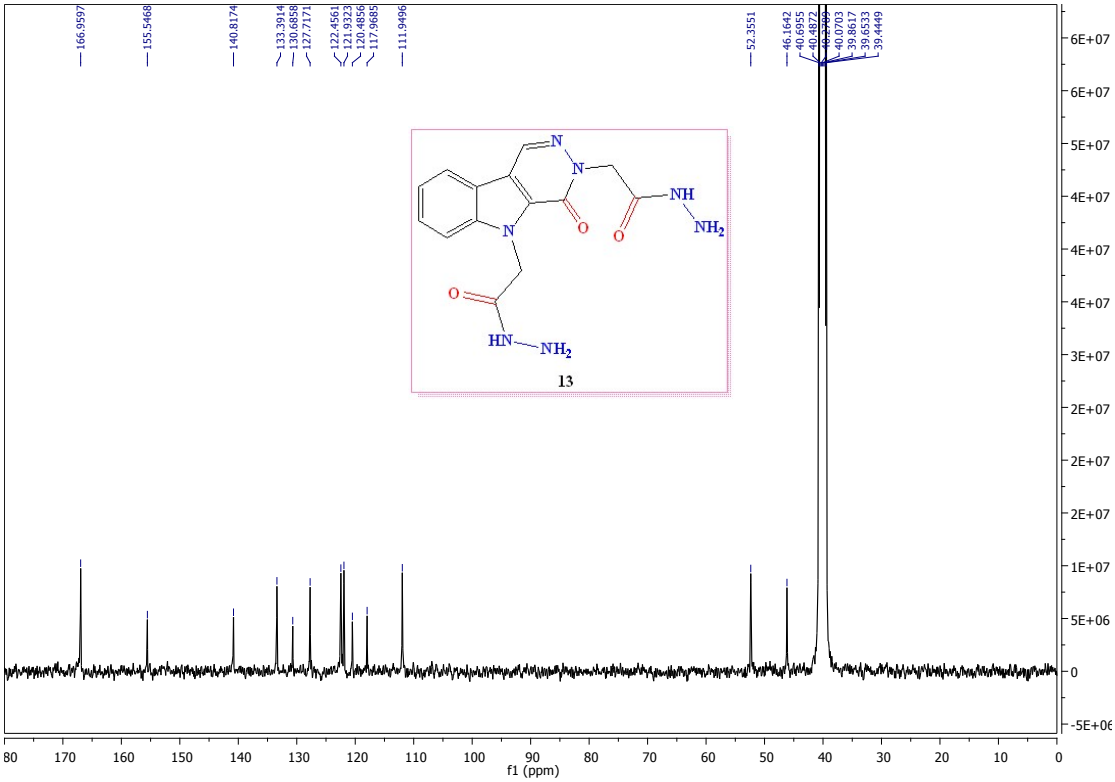

Figure S30: ^{13}CNMR of **13-** DMSO-d_6